

CAMEA—A novel multiplexing analyzer for neutron spectroscopy

Felix Grottl, Dieter Graf, Jonas Okkels Birk, Márton Markó, Marek Bartkowiak, Uwe Filges, Christof Niedermayer, Christian Rüegg, and Henrik M. Rønnow

Citation: [Review of Scientific Instruments](#) **87**, 035109 (2016); doi: 10.1063/1.4943208

View online: <http://dx.doi.org/10.1063/1.4943208>

View Table of Contents: <http://scitation.aip.org/content/aip/journal/rsi/87/3?ver=pdfcov>

Published by the [AIP Publishing](#)

Articles you may be interested in

[A Proton Recoil Telescope Detector for Neutron Spectroscopy](#)

AIP Conf. Proc. **947**, 35 (2007); 10.1063/1.2813831

[Experimental neutron spectroscopy data visualization: Adaptive tessellation algorithm](#)

Rev. Sci. Instrum. **78**, 043901 (2007); 10.1063/1.2722398

[New MPRu instrument for neutron emission spectroscopy at JET](#)

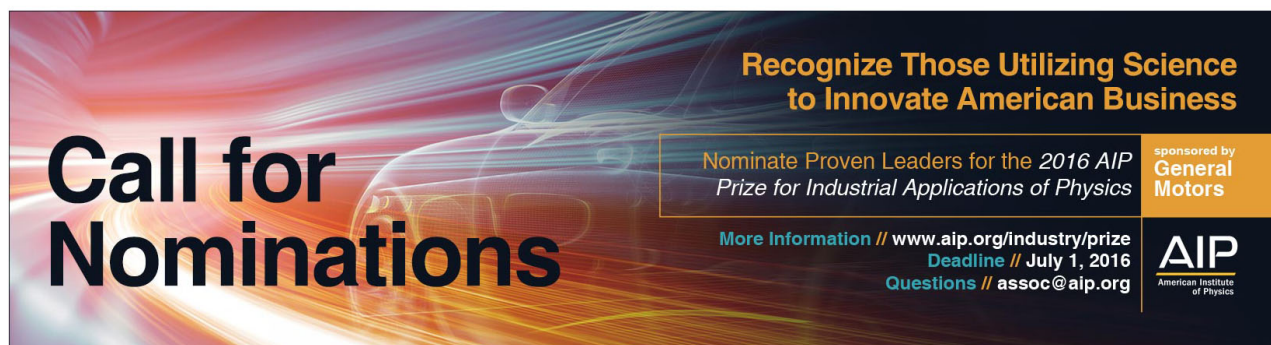
Rev. Sci. Instrum. **77**, 10E717 (2006); 10.1063/1.2336459

[Neutron emission spectroscopy at JET—Results from the magnetic proton recoil spectrometer \(invited\)](#)

Rev. Sci. Instrum. **72**, 759 (2001); 10.1063/1.1321738

[Fusion Neutronic Source deuterium–tritium neutron spectrum measurements using natural diamond detectors](#)

Rev. Sci. Instrum. **68**, 1720 (1997); 10.1063/1.1148001



Call for Nominations

Recognize Those Utilizing Science to Innovate American Business

Nominate Proven Leaders for the *2016 AIP Prize for Industrial Applications of Physics*

More Information // www.aip.org/industry/prize
Deadline // July 1, 2016
Questions // assoc@aip.org

sponsored by
General Motors

AIP
American Institute of Physics

CAMEA—A novel multiplexing analyzer for neutron spectroscopy

Felix Groitl,^{1,2,a)} Dieter Graf,³ Jonas Okkels Birk,² Márton Markó,^{2,4} Marek Bartkowiak,³ Uwe Filges,³ Christof Niedermayer,² Christian Rüegg,^{2,5} and Henrik M. Rønnow^{1,6}

¹*École Polytechnique Fédérale de Lausanne, Laboratory for Quantum Magnetism, 1015 Lausanne, Switzerland*

²*Paul Scherrer Institute, Laboratory for Neutron Scattering and Imaging, 5232 Villigen, Switzerland*

³*Paul Scherrer Institute, Laboratory for Scientific Developments and Novel Materials, 5232 Villigen, Switzerland*

⁴*Wigner Research Centre for Physics, Neutron Spectroscopy Department, 1525 Budapest, Hungary*

⁵*Department of Quantum Matter Physics, University of Geneva, 1211 Geneva, Switzerland*

⁶*University of Copenhagen, Niels Bohr Institute, 2100 Copenhagen, Denmark*

(Received 17 December 2015; accepted 19 February 2016; published online 11 March 2016)

The analyzer detector system continuous angle multiple energy analysis will be installed on the cold-neutron triple-axis spectrometer RITA-2 at SINQ, PSI. CAMEA is optimized for efficiency in the horizontal scattering plane enabling rapid and detailed mapping of excitations. As a novelty the design employs a series of several sequential upward scattering analyzer arcs. Each arc is set to a different, fixed, final energy and scatters neutrons towards position sensitive detectors. Thus, neutrons with different final energies are recorded simultaneously over a large angular range. In a single data-acquisition many entire constant-energy lines in the horizontal scattering plane are recorded for a quasi-continuous angular coverage of about 60°. With a large combined coverage in energy and momentum, this will result in a very efficient spectrometer, which will be particularly suited for parametric studies under extreme conditions with restrictive sample environments (high field magnets or pressure cells) and for small samples of novel materials. In this paper we outline the concept and the specifications of the instrument currently under construction. © 2016 AIP Publishing LLC. [<http://dx.doi.org/10.1063/1.4943208>]

I. INTRODUCTION

In solid state physics the investigation of elementary excitations, such as phonons and magnons, by means of inelastic neutron scattering is a well established method. The dynamic structure factor $S(\mathbf{q}, \omega)$ in the 4D momentum-energy space (\mathbf{q}, ω) is investigated by measuring the energy transfer, $\hbar\omega = E_i - E_f$, and momentum transfer, $\mathbf{q} = \mathbf{k}_f - \mathbf{k}_i$, by comparing the incoming and final neutron energy and momentum, respectively. Such measurements are usually done using time-of-flight (TOF) spectrometers or triple-axis spectrometers (TAS). The advantage of direct TOF spectrometers is a large coverage of (\mathbf{q}, ω) with the caveat of relatively low incoming neutron flux. The large (\mathbf{q}, ω) coverage is achieved by measuring a wide range of scattered energies and simultaneously covering a large solid angle with position sensitive detectors (PSDs). An impressive example is the LET spectrometer at ISIS, UK.¹ However, many experiments include the use of sample environment, such as high field cryo-magnets and pressure cells, which in general restrict the vertical range of scattered neutrons to a few degrees. Thus, using a TOF instrument with such restrictive sample environment reduces the advantage of a large coverage of the (\mathbf{q}, ω) -space, since a large fraction of the PSD area is blocked. Second, while TOF can cover a large (\mathbf{q}, ω) -space, long acquisition times are needed for sufficient statistics in each (\mathbf{q}, ω) -pixel. This

limits the number of measurements that can be performed as a function of an external parameter such as temperature, magnetic field, pressure, etc. (parametric studies). Therefore, such experiments are usually carried out at TAS instruments operating in the horizontal scattering plane. Here, a higher incoming neutron flux is focused to investigate one particular point in (\mathbf{q}, ω) resulting in relatively short counting times. Hence TAS is good for parametric studies but requires long time for mapping.

Since inelastic neutron scattering in general is a flux-limited technique, it is essential to improve the efficiency of spectrometers. For classical TAS instruments this can be achieved by so-called multiplexing, i.e., implementing several (\mathbf{k}_f, E_f) -channels to cover a larger range in (\mathbf{q}, ω) . For analyzing the neutrons in the horizontal scattering plane this results in rather complicated solutions like the RITA spectrometer^{2,3} at Risø, Denmark. Here, the efficiency is increased by “local” multiplexing. Similar realizations are RITA-II^{4,5} at SINQ, Switzerland, UFO^{6,7} and IMPS⁸ at ILL, France, and the multi-analyzer system at PUMA⁹ at FRM II, Germany. For these type of spectrometers the number of possible (\mathbf{k}_f, E_f) -channels is limited due to geometrical restrictions and the overall gain is limited by the analyzer area. Another possibility to overcome these geometrical restrictions and to increase the (\mathbf{q}, ω) coverage is wide-angle multiplexing. This is realized at MADbox^{10,11} at ILL, France, and MACS¹² at NIST, USA. A special realization of the wide-angle multiplexing concept is Flatcone¹³ at ILL, France, since it employs vertically scattering analyzers. These kind

^{a)}Electronic mail: felix.groitl@psi.ch

of instruments are all limited by density of (\mathbf{q}, ω) coverage, since only one final energy is analyzed. Thus, a logic step in progression is to simultaneously increase the number of analyzed final energies, which is realized in the CAMEA concept.

The CAMEA (Continuous Angle Multiple Energy Analysis) concept presented here is a new generation of multiplexing instruments, which makes use of the nearly perfect transmission of highly oriented pyrolytic graphite (HOPG) for cold neutrons,¹⁴ which do not fulfill the Bragg law. This allows to use a series of upward scattering analyzer arcs behind each other fixed to different energies in order to optimize the coverage for in-plane scattering. The scattered neutrons are measured by a detector array consisting of PSDs with a quasi-continuous angular coverage. Thus, the coverage of (\mathbf{q}, ω) is drastically increased and with a simple rotation scan of the sample around its vertical axis several constant energy maps can be produced. This design is an optimal solution to increase the detection efficiency for in-plane scattering and hence is particularly suited for experiments using restrictive sample environments and small sample volumes.

The CAMEA design was successfully proposed for the future European Spallation Source (ESS) where it will be applied as an inverse TOF spectrometer in the high performance BIFROST spectrometer.¹⁵ Recently, other multiplexing instruments exploiting the CAMEA concept were proposed: MultiFLEXX^{16,17} currently in commissioning at HZB, Germany, and BAMBUS¹⁸ considered at FRM II, Germany. The CAMEA design was validated by extensive prototype experiments performed at MARS,¹⁹ SINQ, where a flexible prototype with 3 analyzers and corresponding detector modules was installed. The results of these experiments will be published elsewhere.²⁰ In this paper, design studies and instrument details for the new secondary spectrometer CAMEA currently being constructed at SINQ, PSI, will be presented.

II. INSTRUMENT SPECIFICATIONS

The existing cold neutron TAS RITA-II is located at the neutron guide 1RNR13 (curved guide, super-mirror $m = 2$, cross section 30×120) at the Swiss Spallation Neutron Source (SINQ) with a distance of 42 m to the cold source. The instrument employs a vertically focusing monochromator and can host all standard neutron scattering sample environments, such as cryo-magnets, pressure cells, and low temperature cryostats.

A. Analyzers and detectors

The key design of CAMEA is to use a series of vertically scattering analyzers to select different final energies of the scattered neutrons at the same time (see Fig. 1). By extending the analyzers to arcs, a large coverage for in-plane scattered neutrons can be achieved (see Fig. 2). For the realization of the CAMEA secondary spectrometer at SINQ several boundary conditions had to be taken into account:

1. As for RITA-II the new spectrometer must be able to host the full SINQ sample environment suite.

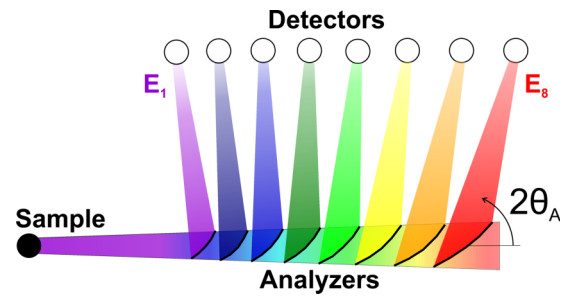


FIG. 1. Simplified sketch of CAMEA. Here, a vertical cut is shown. Neutrons are scattered with different energies by the sample and are selected by a series of upward scattering analyzers with different final energies E_f .

2. The current instrument area of RITA-II is located between two neutron guides limiting the maximum length of the secondary spectrometer.
3. In order to avoid a contamination, i.e., a larger background signal, due to higher order incoming neutron energies scattered by the monochromator, a beryllium filter must be implemented in the secondary neutron flight path. Furthermore, a radial collimator is needed to reduce the background arising from sample environment.

The new instrument will employ 8 fixed E_f -channels in the energy range of 3.2–5 meV (see Table I). The maximum energy of 5 meV is determined by the use of a beryllium filter and its cutoff energy of 5.2 meV. The number of 8 final energies and the corresponding ΔE -acceptance (see Table I) in the chosen range allow for a dense coverage in energy. The choice of a minimum energy of 3.2 meV (with $2\theta_A = 97.8^\circ$) is due to boundary conditions (1) and (2). The smallest achievable distance between the first detector position (see E_1 in Fig. 1) and the vertical sample axis is defined by the dimensions of sample environment (1). Therefore, keeping the detector position and going to lower final energies with an even larger $2\theta_A$ would move the arcs further away from the sample position. Thus, if one wants to keep the dense coverage in energy with the same or even higher number of

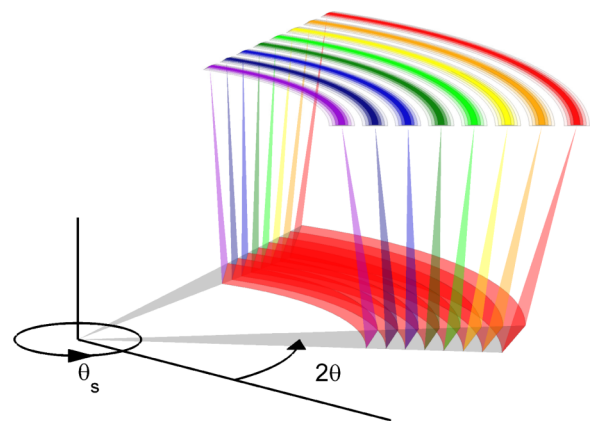


FIG. 2. Simplified sketch of an ideal secondary CAMEA spectrometer. The upward scattering analyzer arcs cover a large range of scattering angles. The analyzed neutrons with different final energies are then detected by a detector array. The instrument is set to a scattering angle 2θ and the sample rotation angle θ_s is scanned.

TABLE I. Detailed specifications of the analyzer segments of the CAMEA spectrometer. Top: Final energies, distances, and dimensions of the segments. Bottom: Results of McStas simulations for the central detector tube. Given are integrated overall intensities, the resolution for the channels (single pixel, two binned pixels, and all pixels of a segment binned), and scattering angle resolution.

	# Analyzer segment							
	1	2	3	4	5	6	7	8
E_f (meV)	3.21	3.38	3.58	3.80	4.05	4.33	4.64	5.01
Sample to analyzer (mm)	930	994	1056	1120	1183	1247	1312	1379
Analyzer to detector (mm)	707	702	700	701	703	709	717	727
HOPG length (mm)	72.0	81.8	91.6	102.4	112.2	119.1	128.1	139.2
Angular coverage (deg)	3.82	4.14	4.42	4.73	4.95	5.19	5.41	5.60
Normalized integrated I (a.u.)	1.00	0.93	0.88	0.86	0.81	0.73	0.75	0.69
1 pixel ΔE_f (FWHM) (μeV)	57.1	62.3	69.3	78.1	85.6	98.5	107.5	116.5
2 pixels ΔE_f (FWHM) (μeV)	63.4	69.8	77.4	87.3	96.9	108.8	120.1	128.1
All pixels ΔE_f (FWHM) (μeV)	94.8	112.6	124.8	132.5	156.1	157.7	197.6	203.4
$\Delta 2\theta$ (FWHM) (Arch Min)	44.2	42.3	39.7	37.6	35.6	33.8	31.7	30.3

arcs, the instrument length would increase and be too long for the available instrument areal (2).

Continuous analyzer arcs as sketched in Fig. 2 are difficult to implement without complex holders, which would limit the transmission throughout the series of arcs. Thus, for CAMEA the arcs are divided into 8 modules. Each module contains 8 analyzer segments fixed to the different final energies (see Fig. 3). The angular span of one module is 7.5° resulting in a total coverage of 60° . The angular span of the module and the Bragg condition of each analyzer segment determine the angular coverage and the length of the analyzer blades of each segment. The angular coverage and the lengths are given in Table I. The angular coverage for the lowest energy is 51% and 75% for the highest energy. Thus, by performing a second measurement with the sample scattering angle 2θ shifted by 3.75° a continuous coverage can be achieved (see Fig. 4).

Taking into account the vertical opening of a typical superconducting cryo-magnet for neutron scattering at SINQ, e.g., $\pm 2^\circ$ for MA15,²¹ a vertical acceptance of $\pm 2^\circ$ was chosen for the analyzer segments. This is achieved by using 5 blades of HOPG per segment. The width of the blades is different for each segment (see Table I) resulting in a total area of HOPG

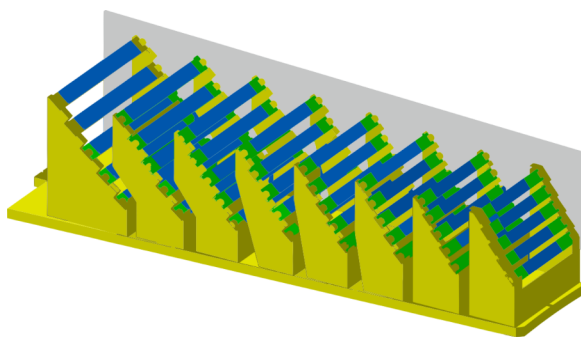


FIG. 3. Design of the analyzer segments of one module. The HOPG crystals (blue) are mounted on Si blades (green), which are fixed within aluminum holders (yellow). The neutrons transmitted through all analyzers are absorbed in a beamstop (not shown). Between each module cross-talk is prevented by Boralcan plates (gray).

of 0.44 m^2 . The HOPG blades (mosaicity of $60' = 1^\circ$ FWHM) are mounted on Si wafers within an aluminum frame. The Si wafers have an excellent transmission for cold neutrons and produce almost no background. A thickness of 1 mm was chosen for the HOPG crystals. This ensures a transmission of $>98\%$ ¹⁵ and compared to a typically used thickness of 2 mm, the costs are halved by sacrificing only a small amount of reflectivity. The Si wafers with the HOPG are placed in a focusing Rowland geometry.²² In combination with the relaxed mosaicity of the HOPG crystals this allows to apply the so-called prismatic analyzer concept.²³ This concept will be discussed in Subsection II B.

The scattered neutrons are detected by linear position sensitive He^3 detector tubes ($\phi = 0.5 \text{ in.}$), which are mounted radially. In order to minimize the gaps between the single detector tubes for the higher E_f -channels, the detectors are mounted in two layers above each other (see Fig. 5), where each detector has an active length of 90.4 cm. Following the modular design of the analyzers, the detectors are likewise

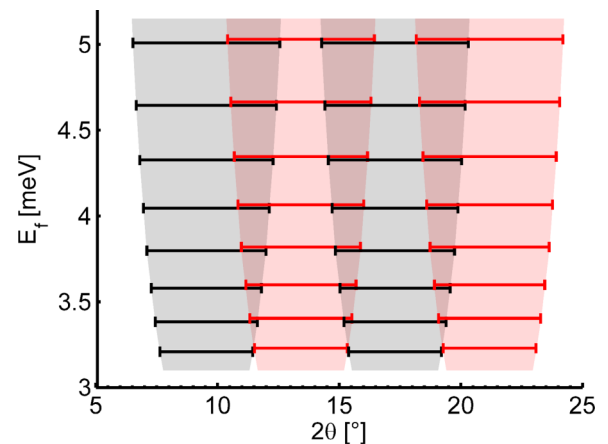


FIG. 4. Angular coverage of two neighboring analyzer segments for two sample scattering angles, 2θ (black) and $2\theta + 3.75^\circ$ (red). For the first analyzer segment at $E_f = 3.2 \text{ meV}$ there is almost no overlap between the two measurements while the overlap increases to 2/3 for the last analyzer segment at $E_f = 5 \text{ meV}$.

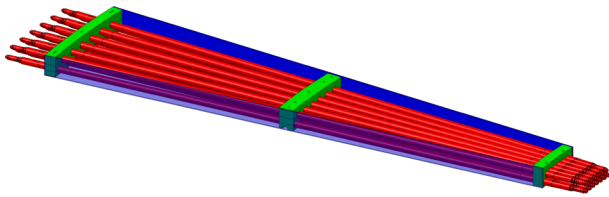


FIG. 5. Design drawing of one detector module. The module consists of 13 He^3 position sensitive detector tubes ($\phi=0.5$ in.), which are mounted radially in two layers.

mounted in modules. Here, each module hosts 13 detector tubes covering the angular span of 7.5° . This gives a total number of 104 detector tubes. The radial detector design implies that the q -channel is defined by the tube, while the final energy of the scattered neutron is defined by the position along the detector tube. The expected spatial resolution along the detector tube is $\sim 1\%$ of the active length, which is in excellent agreement with the resolution of ~ 8 mm experimentally obtained in a test setup. In the practical implementation the neutrons are recorded into pixels with a length of ~ 2 mm. The length of these pixels is determined by the resolution of the used electronics. For simplicity, for the remainder the functioning will be discussed in terms of pixels, where the pixel length equals the positional resolution.

B. Resolution and coverage

CAMEA applies the prismatic analyzer concept²³ (see Fig. 6). Here, the analyzer blades are oriented in a focusing Rowland geometry.²² Combining distance collimation (distances see Table I) and a relaxed analyzer mosaicity of $60'$ allows for each analyzer segment to record a range of energies in the corresponding detector pixels. In combination this improves the energy resolution and the overall count rate compared to using analyzers with a smaller mosaicity. In the course of the prototype measurements²⁰ the analytically calculated high energy resolution²⁴ was verified.

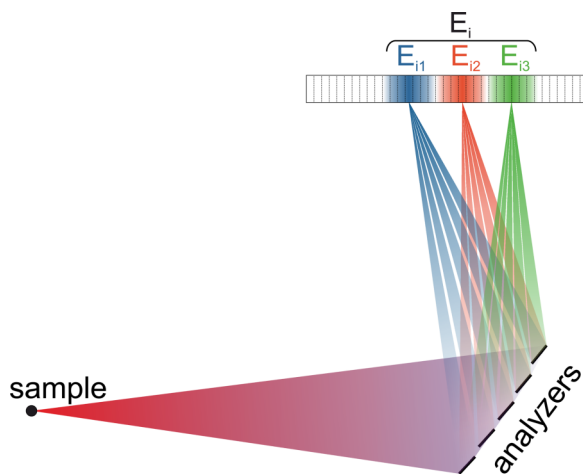


FIG. 6. Sketch of the prismatic analyzer concept. Five analyzer blades are oriented in a focusing Rowland geometry. Due to the relaxed mosaicity ($60'$) and distance collimation, the slightly different reflected energies represented by the different coloring are clearly separated and detected in the pixels of the position sensitive detector.

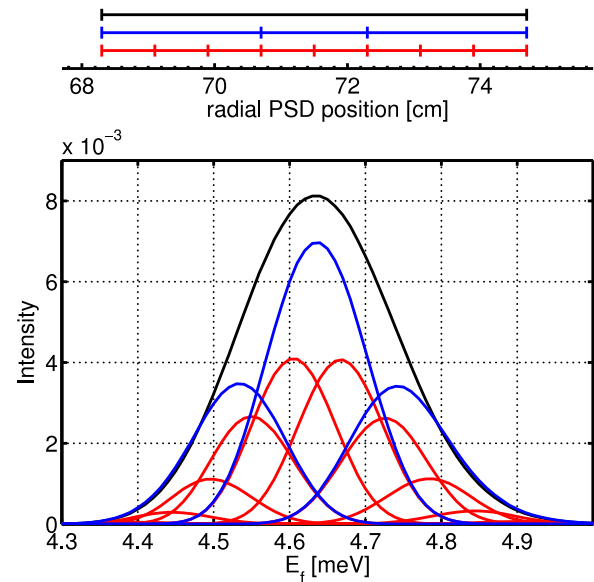


FIG. 7. Simulated elastic intensities from the 7th analyzer segment along one PSD tube plotted as a function of E_f . The peak energy for the different pixels (red) is slightly shifted due to the prismatic analyzer. By binning pixels (blue) the intensity can be increased while slightly worsening the energy resolution. The integrated intensity is shown by the black line. The pixel position along the PSD tube for the different binnings is sketched above.

For CAMEA the calculated resolution for one pixel is $\Delta E_f(FWHM)/E_f \approx 1.8\% - 2.3\%$ (see Table I). The overall resolution is determined by the convolution of the primary and secondary spectrometer energy resolution and typically 10%-20% better than a standard TAS.

In order to optimize the analyzer segments and determine the resolution, simulations were performed using the neutron ray-tracing Monte Carlo package McStas.^{25,26} The existing RITA-II instrument description,²⁷ which has proven to model the instrument well, was used. The instrument description was then adapted for the new CAMEA analyzer system. Fig. 7 shows for the 7th analyzer segment the simulated elastic intensity for the detector pixels of one PSD tube as a function of final energy (red). Due to the prismatic analyzer the peak energy of each pixel is slightly shifted with an amplitude that decreases away from the central energy due to the finite mosaicity of the analyzer crystals. During analysis after the experiment it is now possible to compromise between resolution and statistics by either keeping each pixel separate (red), binning 2 pixels (blue), or binning all pixels (black).

The integrated simulated intensity as a function of final energy for all analyzer segments is shown in Fig. 8 demonstrating the quasi-continuous energy coverage. The results of the simulations for one detector tube, i.e., integrated overall intensities, the resolution for the different channels (single pixel, two binned pixels, and all pixels of a segment binned) and scattering angle resolution is summarized in Table I.

Taking the number of analyzer segments and detector tubes and assuming that the detector pixels are binned in pairs so that 3 final energies are investigated per analyzer segment (see Fig. 7, blue), a total number of 2496 points in

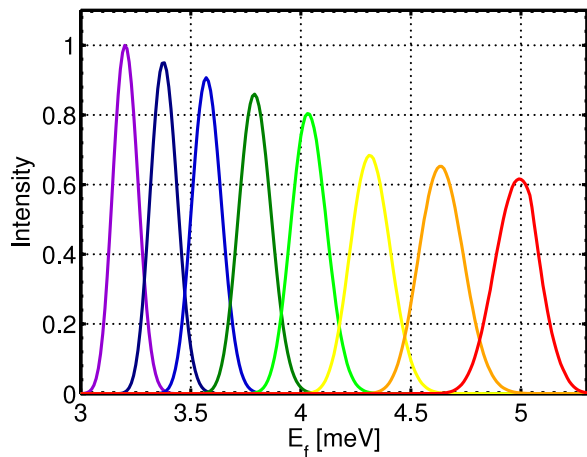


FIG. 8. Integrated simulated elastic intensities for all 8 analyzer segments as a function of E_f . The results demonstrate the quasi-continuous energy coverage of the spectrometer.

$S(\mathbf{q}, \omega)$ is measured simultaneously. By a simple rotation scan of the sample (θ_s , see Fig. 2) with the instrument fixed to one scattering angle 2θ , constant energy maps are produced. Performing the sample rotation scan for two scattering angles (2θ and $2\theta + 3.75^\circ$) provides a continuous coverage of the reachable (\mathbf{q}, ω) -space as shown in Fig. 9. Here, only 15 scan steps are plotted for visibility. In Fig. 10 we illustrate the data that will be obtained from an 81 step sample rotation for a material hosting 2D AFM spin waves with one boundary of 2 meV (not accounting for quantum effects²⁸). For visibility all 24 energies are only shown in the outermost dispersion cone. For the rest of the maps only the central energy of each analyzer segment is plotted.

Another measurement option is a θ_s - θ -scan, where the scattering angle (2θ) is changed by the same amount as the sample angle (θ_s).¹⁶ This kind of scan allows a more focused measurement in momentum-space.

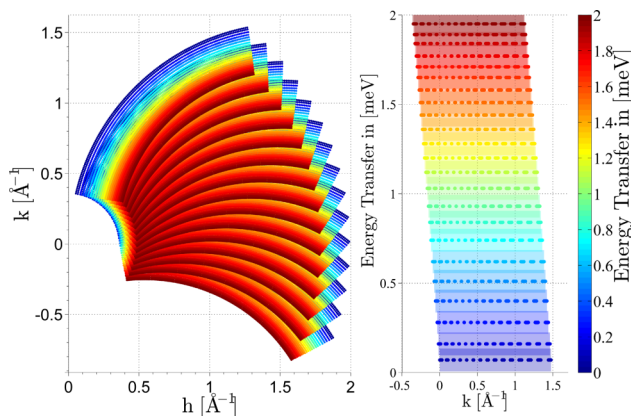


FIG. 9. Example for (\mathbf{q}, ω) -space covered by a sample rotation scan. Left: 15 rotation steps (step size 5°) for two scattering angles (2θ and $2\theta + 3.75^\circ$) and $E_f = 5.2$ meV were calculated using a cubic sample ($a = 2\pi$ Å). For every step a total number of 2496 data points is measured. Right: Energy transfer covered by data points along the $(1\ k\ 0)$ -axis. The FWHM for the different energy transfers for a 2 pixel binning as given in Table 1 is shown by rectangles.

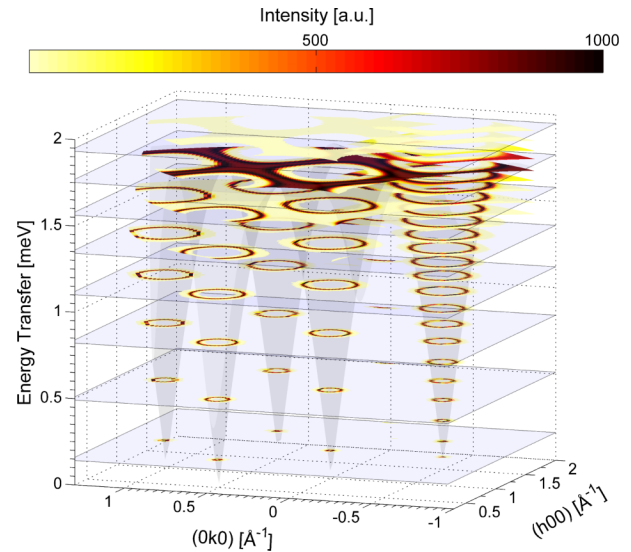


FIG. 10. Calculated intensity for a typical spin wave excitation covered by an 81 step scan (step size 1°) with the same parameters as used in Fig. 9. Here, for visibility all 24 energies are only shown in the outermost cone. For the rest of the data only the maps from the central energy of each analyzer segment are shown.

C. Filter and collimator

The instrument is optimized for the use of complex sample environment, which causes a source of background. For instance, cryo-magnets are stabilized by concentric aluminum rings around the sample position. Therefore, due to the rather open design of CAMEA, a radial collimator is needed to remove the background arising from the sample environment. Due to the dimensions of the sample environment available at SINQ, the collimator needs at least a distance of 550 mm to the sample. Taking design boundary condition (2) into account, a maximum length of 280 mm is possible. As a compromise between transmission and focal width, an angular opening of 1° was chosen. Simultaneously the instrument needs a beryllium filter. Since the beamline does not employ a velocity selector, the analyzed signal would be contaminated by $\lambda/2$ neutrons scattered by the monochromator and the sample. This would not only affect the analyzed signal but also increase the background in the detector tubes.¹⁷ For higher neutron energies the analyzer crystals will not only scatter from (00l) but also from (hkl) type reflections²⁹⁻³¹ and increase the background in the front channels. For a 10^{-3} suppression of $\lambda/2$ neutrons, a Be filter length of 120 mm is necessary.³² At the same time this device needs to be cooled to liquid nitrogen temperatures in order to improve its transmission.^{33,34} Due to the spatial restrictions and to remove diffusive leakage through the Be the two devices, radial collimator and Be filter, are combined and both dry cooled in vacuum using a conventional Gifford-McMahon cooling head. This is especially challenging due to the different thermal expansion coefficients of the used materials. The lamellae of the collimator are much longer than the beryllium and the stack cannot be pressed together but must be mounted separately in a housing. Thus, the thermal contraction has to be taken into account by simultaneously ensuring a good thermal contact

between housing and beryllium. Such a combined device was successfully built and tested at PSI.³⁵

D. Shielding

For any spectrometer a good background reduction is crucial. The secondary spectrometer will be completely in vacuum in order to reduce the background from air scattering. The vacuum solution was chosen, since it simultaneously makes an additional housing for the cooled filter-collimator redundant. According to Paschen law, the breakdown voltage of the alternative argon at atmospheric pressure for a typical distance of 10 mm is exceeded for a vacuum of <0.1 mbar. Thus, going to pressures of type 10^{-4} mbar the spatial restrictions on the signal feedthroughs are much more relaxed. The tank will then be thoroughly shielded against the general background present in the SINQ guide hall. Prototype results suggest that this will produce low inelastic background in the order of 10^{-4} compared to the elastic signal from vanadium.²⁰ The inner part of the secondary spectrometer is shown in detail in Fig. 11. To remove background arising from crosstalk between the different analyzer segments a shielding framework is installed between analyzers and detectors. Furthermore, any non-absorbing surface will be covered with neutron absorbing material such as BORALCAN and BORAL.

A design drawing of the full CAMEA spectrometer is shown in Fig. 12. The existing monochromator part of RITA-II (green) is preserved while the sample table (light blue) is only adapted to the increased weight of the secondary spectrometer (an upgrade with optimized guides³⁶ is envisaged later). The substructure (orange) of the secondary spectrometer is mounted on air pads and hosts all electronics, the vacuum pump, and the cooling head. A cut through the vacuum tank (yellow) is shown. The tank will be covered in borated polyethylene as a shielding against the general background in the SINQ guide hall.

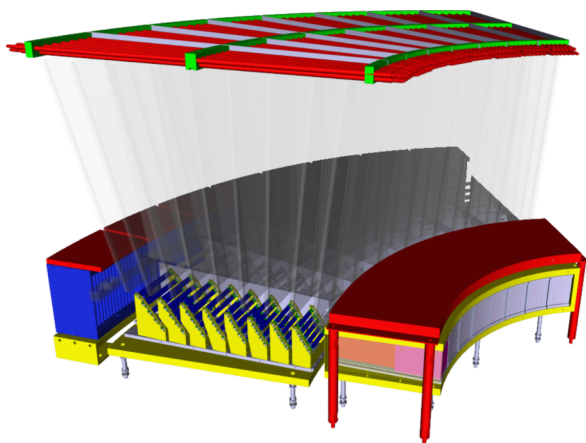


FIG. 11. Full design drawing of the inner parts of the CAMEA vacuum tank. The combined Be-filter-collimator (Be (purple) and lamellas (orange), right), the analyzer segments (yellow/blue, bottom), and the beamstop (blue, left) are mounted on a base plate. The filter and the beamstop are shielded towards the detectors (dark red). The crosstalk shielding is mounted between the analyzers and the detectors (gray, semi-transparent). Two layers of PSD tubes (red, top) are mounted on the lid of the vacuum tank.

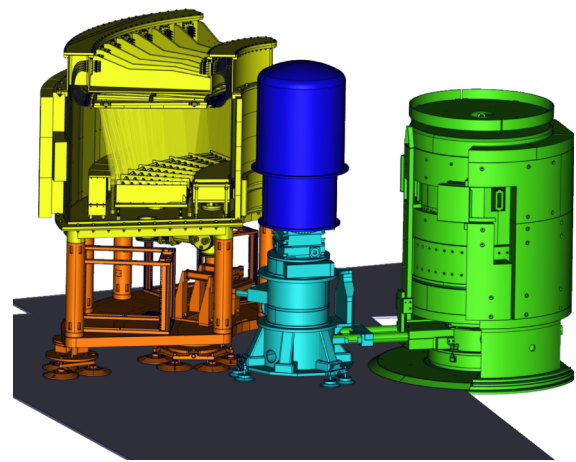


FIG. 12. Design drawing of the CAMEA spectrometer. The monochromator part (green) and sample table (light blue) are preserved while the secondary spectrometer (substructure (orange) and vacuum vessel (yellow)) are newly constructed. The vessel is thoroughly shielded against general background in the guide hall. The inner part of the vessel is shown in detail in Fig. 11.

III. CONCLUSION

CAMEA introduces a novel class of neutron spectrometers especially suited for parametric studies under extreme conditions using sample environment with restrictive scattering geometries. The instrument is currently under construction at SINQ, PSI, and critical parts of the instrument have been examined by thorough prototyping and simulations. Using several concentric analyzer arcs and prismatic analyzers, the CAMEA design allows to cover a large region in momentum-energy-space within a single data-acquisition resulting in substantial gains in data collection rates.

ACKNOWLEDGMENTS

The authors would like to thank Raphael Müller, Peter Keller, Urs Greuter, Christian Kägi, and Emmanouela Rantsiou for technical support. This project is supported by the Swiss National Science Foundation within R'Equip Grant No. 206021-144972.

¹R. I. Bewley, J. W. Taylor, and S. M. Bennington, *Nucl. Instrum. Methods Phys. Res., Sect. A* **637**, 128 (2011).

²T. E. Mason, K. N. Clausen, G. Aeppli, D. F. McMorrow, and J. K. Kjems, *Can. J. Phys.* **73**, 697 (1995).

³K. N. Clausen, D. F. McMorrow, K. Lefmann, G. Aeppli, T. E. Mason, A. Schroder, M. Issikii, M. Nohara, and H. Takagi, *Physica B* **241**, 50 (1997).

⁴K. Lefmann, D. F. McMorrow, H. M. Rønnow, K. Nielsen, K. N. Clausen, B. Lake, and G. Aeppli, *Physica B* **283**, 343 (2000).

⁵K. Lefmann, C. Niedermayer, A. B. Abrahamsen, C. R. H. Bahl, N. B. Christensen, H. S. Jacobsen, T. L. Larsen, P. Haefliger, U. Filges, and H. M. Rønnow, *Phys. B* **385-386**, 1083 (2006).

⁶W. Schmidt, M. C. Rheinstaedter, S. Raymond, and M. Ohl, *Phys. B* **350**, E849 (2004).

⁷W. Schmidt and M. Ohl, in *8th International Conference on Neutron Scattering, Sydney, Australia, 27 November–02 December 2005* [*Phys. B* **385-386**, 1073 (2006)].

⁸M. Jimenez-Ruiz, A. Hiess, R. Currat, J. Kulda, and F. J. Bermejo, *Phys. B* **385-386**, 1086 (2006).

⁹O. Sobolev, R. Hoffmann, H. Gibhardt, N. Jnke, A. Knorr, V. Meyer, and G. Eckold, *Nucl. Instrum. Methods Phys. Res., Sect. A* **772**, 63 (2015).

¹⁰F. Demmel, A. Fleischmann, and W. Glaser, *Nucl. Instrum. Methods Phys. Res., Sect. A* **416**, 115 (1998).

- ¹¹F. Demmel, N. Grach, and H. M. Rønnow, *Nucl. Instrum. Methods Phys. Res., Sect. A* **530**, 404 (2004).
- ¹²J. A. Rodriguez, D. M. Adler, P. C. Brand, C. Broholm, J. C. Cook, C. Brocker, R. Hammond, Z. Huang, P. Hundertmark, J. W. Lynn, N. C. Maliszewskij, J. Moyer, J. Orndorff, D. Pierce, T. D. Pike, G. Scharfstein, S. A. Smee, and R. Vilaseca, *Meas. Sci. Technol.* **19**, 034023 (2008).
- ¹³M. Kempa, B. Janousova, J. Saroun, P. Flores, M. Boehm, F. Demmel, and J. Kulda, *Phys. B* **385-386**, 1080 (2006).
- ¹⁴J. Larsen, Epfl-Report-190504, <http://infoscience.epfl.ch/record/190504?ln=en>, 2014.
- ¹⁵P. G. Freeman, J. O. Birk, M. Marko, M. Bertelsen, J. Larsen, N. B. Christensen, K. Lefmann, J. Jacobsen, C. Niedermayer, F. Juranyi, and H. M. Rønnow, in *QENS/WINS 2014 - 11th International Conference on Quasielastic Neutron Scattering and 6th International Workshop on Inelastic Neutron Spectrometers*, edited by B. Frick, M. Koza, M. Boehm, and H. Mutka, EPJ Web of Conferences Vol. 83 (EDP Sciences, 2015).
- ¹⁶K. Habicht, D. L. Quintero-Castro, R. Toft-Petersen, M. Kure, L. Maede, F. Groitl, and M. D. Le, in *QENS/WINS 2014 - 11th International Conference on Quasielastic Neutron Scattering and 6th International Workshop on Inelastic Neutron Spectrometers*, edited by B. Frick, M. Koza, M. Boehm, and H. Mutka, EPJ Web of Conferences Vol. 83 (EDP Sciences, 2015).
- ¹⁷R. Toft-Peterson, F. Groitl, D. Quintero-Castro, M. Kure, J. Lim, P. Cernak, S. Alimov, T. Wilpert, M. D. Le, C. Niedermayer, A. Schneidewind, and K. Habicht, "The first prototype tests of the vertically scattering multiple energy analysis backend for cold triple axis spectrometers," *Nucl. Instrum. Methods Phys. Res., Sect. A* (to be published).
- ¹⁸J. A. Lim, K. Siemsmeyer, P. Cermak, B. Lake, A. Schneidewind, and D. S. Inosov, in *International Conference on Strongly Correlated Electron Systems 2014 (SCES2014)*, edited by M. Zhitomirsky and P. DeReotier, Journal of Physics Conference Series Vol. 592 (IOP Publishing LTD, 2015).
- ¹⁹P. Tregenna-Piggott, F. Juranyi, and P. Allenspach, *J. Neutron Res.* **16**, 1 (2008).
- ²⁰M. Markó, F. Groitl, J. O. Birk, P. G. Freeman, K. Lefmann, N. B. Christensen, C. Niedermayer, F. Jurányi, A. Hansen, and H. M. Rønnow, "Prototype of the novel CAMEA concept—A backend for neutron spectrometers" (to be published).
- ²¹See <http://www.psi.ch/ldm/sample-environment> for information on dimensions and specifications of existing sample environment at PSI.
- ²²M. Skoulatos, K. Habicht, and K. Lieutenant, *5th European Conference on Neutron Scattering*, Journal of Physics Conference Series Vol. 340 (IOP Publishing LTD, 2012).
- ²³J. O. Birk, M. Marko, P. G. Freeman, J. Jacobsen, R. L. Hansen, N. B. Christensen, C. Niedermayer, M. Mansson, H. M. Rønnow, and K. Lefmann, *Rev. Sci. Instrum.* **85**, 113908 (2014).
- ²⁴M. Markó, Analytical calculations for CAMEA, <http://infoscience.epfl.ch/record/190497?ln=en>, 2014.
- ²⁵K. Lefmann and K. Nielsen, *Neutron News* **10**, 20 (1999).
- ²⁶P. Willendrup, E. Farhi, and K. Lefmann, *Phys. B* **350**, E735 (2004).
- ²⁷L. Udby, P. K. Willendrup, E. Knudsen, C. Niedermayer, U. Filges, N. B. Christensen, E. Farhi, B. O. Wells, and K. Lefmann, *Nucl. Instrum. Methods Phys. Res., Sect. A* **634**, S138 (2011).
- ²⁸B. D. Piazza, M. Mourigal, N. B. Christensen, G. J. Nilsen, P. Tregenna-Piggott, T. G. Perring, M. Enderle, D. F. McMorrow, D. A. Ivanov, and H. M. Rønnow, *Nat. Phys.* **11**, 62 (2015).
- ²⁹E. Frikkee, *Nucl. Instrum. Methods* **125**, 307 (1975).
- ³⁰M. Adib, N. Habib, and M. Fathaalla, *Ann. Nucl. Energy* **33**, 627 (2006).
- ³¹M. Adib, N. Habib, I. Bashter, and A. Saleh, *Ann. Nucl. Energy* **38**, 802 (2011).
- ³²F. J. Webb, *Nucl. Instrum. Methods* **69**, 325 (1969).
- ³³D. C. Tennant, *Rev. Sci. Instrum.* **59**, 380 (1988).
- ³⁴N. Habib, *J. Nucl. Radiat. Phys.* **1**, 137 (2006).
- ³⁵F. Groitl, E. Rantsiou, M. Bartkowiak, U. Filges, D. Graf, C. Niedermayer, C. Rüegg, and H. M. Rønnow, "Performance of a combined radial collimator and cooled Be filter," *Nucl. Instrum. Methods Phys. Res., Sect. A* (published online).
- ³⁶K. Lefmann, U. Filges, F. Treue, J. J. K. Kirkensgaard, B. Plesner, K. S. Hansen, and K. H. Kleno, *Nucl. Instrum. Methods Phys. Res., Sect. A* **634**, S1 (2011).